

Electron traps in Ga(As,N) layers grown by molecular-beam epitaxy

P. Krispin^{a)}

Paul-Drude-Institut für Festkörperelektronik, Hausvogteiplatz 5-7, 10117 Berlin, Germany

S. G. Spruytte and J. S. Harris

Solid State and Photonics Laboratory, Stanford University, Stanford, California 94305

K. H. Ploog

Paul-Drude-Institut für Festkörperelektronik, Hausvogteiplatz 5-7, 10117 Berlin, Germany

(Received 8 August 2001; accepted for publication 23 January 2002)

Deep levels in the upper half of the band gap of strained Ga(As,N) with a GaN mole fraction of 3% are examined by deep-level transient Fourier spectroscopy on GaAs/Ga(As,N)/GaAs heterojunctions grown by molecular-beam epitaxy. In as-grown structures, we find a dominant electron trap at 0.25 eV below the conduction bandedge with a concentration above 10^{17} cm^{-3} . Its capture cross section of about 10^{-17} cm^2 for electrons is too small for an efficient nonradiative recombination center in Ga(As,N). According to theoretical predictions, this level is most likely connected with a nitrogen-split interstitial defect $(\text{N}-\text{N})_{\text{As}}$. The giant concentration of this trap can be strongly reduced by rapid thermal annealing. © 2002 American Institute of Physics.

[DOI: 10.1063/1.1463214]

Group-III-arsenide-nitrides grown on GaAs substrates are promising materials for optoelectronic devices. Ga(As,N) layers are of special interest, because the band gap is drastically reduced by increasing the GaN mole fraction.¹ In contrast to the optical properties, the electrical characteristics of Ga(As,N) layers have hardly been studied. We have recently shown that GaAs/Ga(As,N) interfaces with a GaN composition of 3% exhibit a conduction band offset ΔE_C of -400 meV .² For the same composition, the valence band offset ΔE_V has been found to be $+11 \text{ meV}$.³ The Ga(As,N)/GaAs heterointerface is therefore of type I.

Crystal quality and luminescence efficiency of Ga(As,N) layers deteriorate for larger GaN mole fractions. Both can be remarkably improved by postgrowth heat treatment.⁴⁻⁷ However, the degradation and anneal mechanisms are still controversially discussed. Nitrogen-related deep-level defects in Ga(As,N) have been proposed as nonradiative recombination centers,^{4,5,7} but not explored yet. We have previously shown that the electronic states found in the lower half of the Ga(As,N) band gap are not due to N-related defects.⁸

In this letter, we use metal-semiconductor (MS) contacts and deep-level transient Fourier spectroscopy (DLTFS)⁹ on *n*-type GaAs/Ga(As,N)/GaAs heterojunctions grown by molecular-beam epitaxy (MBE) to search for electron traps in the upper half of the Ga(As,N) band gap. Details of the epitaxial growth and of the carrier distribution in the investigated samples have been published elsewhere.^{2,7} For as-grown Ga(As,N) with a GaN mole fraction of 3%, we find an electron trap with a giant density at 0.25 eV below the conduction bandedge E_C . According to theoretical predictions, the level is probably associated with the nitrogen-split interstitial defect $(\text{N}-\text{N})_{\text{As}}$ on an As site. Its concentration can be drastically reduced by rapid thermal annealing for 60 s at 760 °C.

For an as-grown GaAs/Ga(As,N)/GaAs structure, deep-level spectra are plotted in Fig. 1 for varying bias conditions. Below 250 K, the presence of a dominant electron trap labeled Ek1 is obvious in Fig. 1(a). Its peak position is constant at low reverse biases (curves 1-3) and shifts to higher temperatures for higher reverse biases. For biases of -5.5 and -6 V (curves 8 and 9), the trap Ek1 is found as a weak signal at 220 K [see the vertical dashed line in Fig. 1(b)]. It disappears at a bias of -6.5 V (curve 10). The thermal acti-

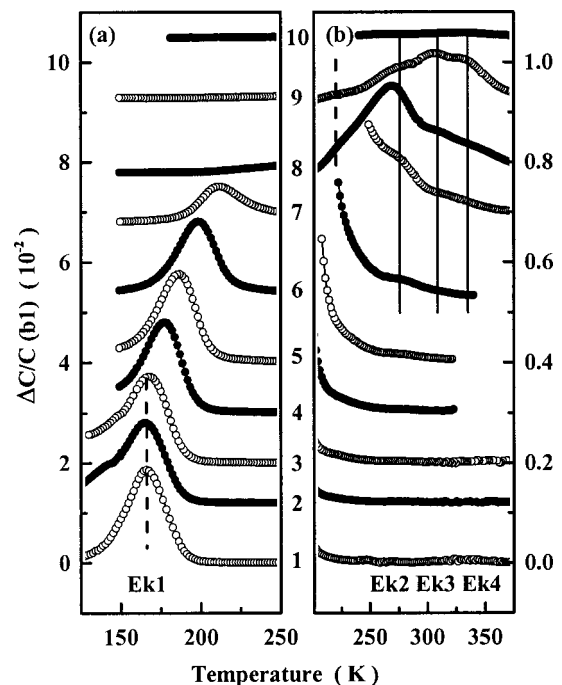


FIG. 1. Typical temperature scans of the DLTFS signal $\Delta C/C$ for as-grown *n*-type GaAs/Ga(As,N)/GaAs heterostructures (Fourier coefficient b_1 , 1 MHz frequency, 1 s period, 100 ms pulse width). The spectra 1-10 correspond from -2 to -6.5 V to reverse biases increasing in 0.5 V steps with a pulse height of 0.5 V. The peak positions of the traps Ek1-Ek4 are indicated. The $\Delta C/C$ scale in (b) is expanded by a factor of 10.

^{a)}Electronic mail: krispin@pdi-berlin.de

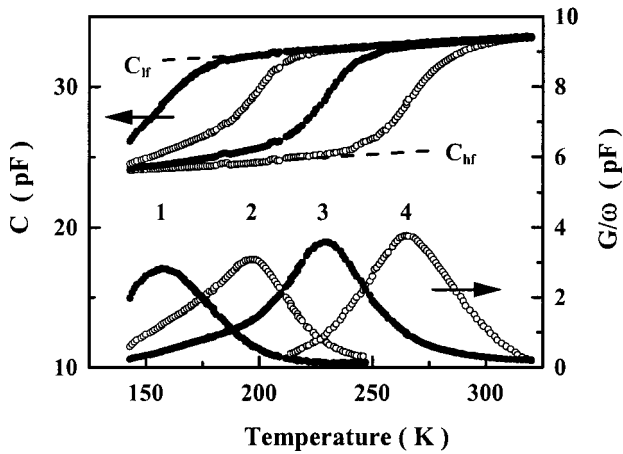


FIG. 2. Typical admittance dispersion for *n*-type GaAs/Ga(As,N)/GaAs structures measured at -2 V and frequencies of (1) 1, (2) 10, (3) 100, and (4) 1000 kHz. The capacitances C_{lf} and C_{hf} are indicated.

vation energy E_t of the level Ek1 changes from 0.25 (curve 1) to about 0.55 eV (curve 9). This tendency is in contrast to an electric-field induced reduction of E_t . In the high reverse-bias range, three minor electron traps Ek2, Ek3, and Ek4 emerge with energies of about 0.62 eV, 0.67 eV, and 0.75 eV, respectively. They also disappear at even higher reverse biases [curve 10 in Fig. 1(b)].

To determine the spatial origin of measured DLTFs responses, their locations below the MS contact are commonly calculated from the voltage-dependent capacitance $C = \epsilon \epsilon_0 A / W$, where W denotes the thickness of the space-charge layer, A the contact area, and $\epsilon \epsilon_0$ the dielectric constant. However, in the bias range from -2 to -4 V, we find a striking admittance dispersion. Capacitance C and ac conductance G/ω depend not only on the bias voltage, but also on temperature (see Fig. 2) and angular frequency $\omega = 2\pi f$ (not shown). The admittance dispersion is characterized by a temperature-dependent time constant $\tau(T_m) = [2\pi f(T_m)]^{-1}$, where $f(T_m)$ is the measuring frequency for the G/ω maximum in Fig. 2 at temperature T_m . Low (lf) and high (hf) frequency conditions are realized for $\omega \ll \tau^{-1}$ and $\omega \gg \tau^{-1}$, respectively. The capacitance in Fig. 2 changes from the lf value C_{lf} to the hf value C_{hf} .

The admittance dispersion is due to the diffusion barriers at the GaAs/Ga(As,N) interfaces, which originate from the relatively large conduction band offset of 400 meV.² The potential distribution around the Ga(As,N) layer is displayed in Fig. 3. The band diagrams have been obtained from simulations of capacitance versus voltage measurements on the as-grown sample of Fig. 1 (see Ref. 2). In particular, the dots in Fig. 3 mark for each bias the thickness W_{lf} obtained from C_{lf} . In the bias range between -2 and -3 V, the measured lf capacitance is dominated by electrons in the Ga(As,N) layer. These electrons can not follow the ac test signal for $\omega \gg \tau^{-1}$, and their contribution to the capacitance is therefore missing at high frequencies and low temperatures. The capacitance C_{hf} is therefore determined by the edge of the depletion layer in the bottom GaAs layer at W_{hf} , which is marked in Fig. 3 by a vertical dashed line. The experimental data in Fig. 2 are completely explained by a simple model,

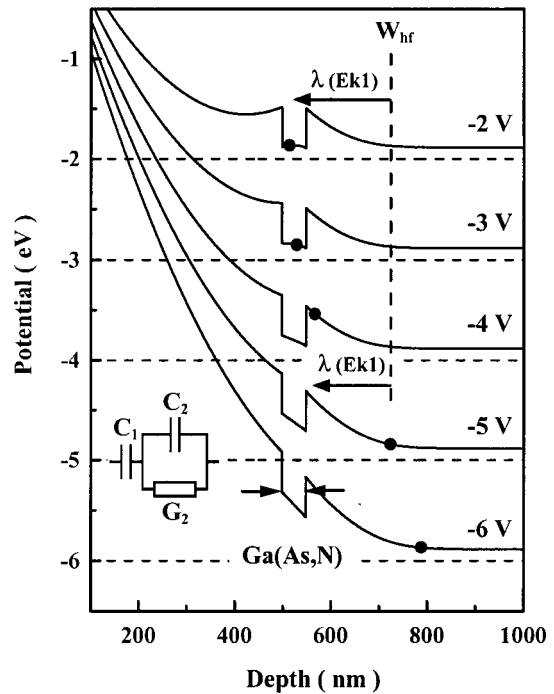


FIG. 3. Band diagram of the *n*-type GaAs/Ga(As,N)/GaAs structures investigated as obtained from solutions of the Poisson equation for several reverse biases. The Fermi level for each bias is given by a horizontal dashed line. Dots mark for each bias the thickness W_{lf} obtained from the capacitance C_{lf} . The depth W_{hf} , which is determined by the edge of the depletion layer in the bottom GaAs layer, is marked by the vertical dashed line. For level Ek1, the λ corrections are indicated by arrows at -2 and -5 V. The electrical equivalent circuit, which explains the admittance dispersion, is sketched in the inset.

which takes into account a series equivalent circuit of two admittances (see inset of Fig. 3), where C_1 and $(C_1^{-1} + C_2^{-1})^{-1}$ are the capacitance values of the MS contact measured under lf and hf conditions, respectively.

The DLTFs response of the electron trap Ek1 in Fig. 1 is measured at 1 MHz and observed below 250 K, i.e., on the hf side of the admittance dispersion (cf. curve 4 in Fig. 2). The signal of the trap Ek1 is thus related to the capacitance C_{hf} and originates because of the λ -effect¹⁰ from the position $(W_{hf} - \lambda)$ below the MS contact, where the Fermi level E_F crosses the deep-level Ek1 at $E_C - 0.25$ eV. Including the band offset, the λ -correction for the level Ek1 is about 200 nm (see in Fig. 3 the arrow at -2 V). We can therefore conclude that the dominant trap at $E_C - 0.25$ eV is located in the Ga(As,N) layer. As long as electrons are present in the Ga(As,N) layer, the peak position and height of the Ek1 signal remain constant between -2 and -3 V [curves 1–3 in Fig. 1(a)]. Using Eq. (4) of Ref. 10, its concentration is estimated from the peak height to be above $1 \times 10^{17} \text{ cm}^{-3}$.

In the bias range from -3 to -5 V, the capacitive contribution of the electrons in the Ga(As,N) layer becomes weaker, and C_{hf} approaches C_{lf} , i.e., the dispersion disappears. The dots in Fig. 3 therefore move toward the vertical dashed line. For the level Ek1 at $E_C - 0.49$ eV detected at -5 V [curve 7 in Fig. 1(a)], the λ -correction is about 180 nm (see in Fig. 3 the arrow at -5 V). In this bias range, the DLTFs peaks of the electron trap Ek1 originate from the interface region, where the GaN mole fraction decreases with

increasing depth. We observe a striking increase of the level energy E_t from 0.25 to about 0.55 eV and a decrease of the trap concentration by two orders of magnitude (see, curves 4–9 in Fig. 1). Likewise, the capture cross section for electrons dramatically increases from 10^{-17} to 10^{-13} cm². From secondary ion mass spectrometry measurements on the investigated structures, we know that the GaN mole fraction in the MBE-grown samples decreases at the Ga(As,N)-on-GaAs interface from 3% to a plateau of 0.2%, which is caused by the operation of the rf plasma cell.⁸ A certain N flux apparently bypasses the closed shutter of the N cell. The aforementioned changes of the level properties are therefore related to the composition range between 3% and 0.2%.

As-grown Ga(As,N) layers contain a significant concentration of interstitial nitrogen,¹¹ in agreement with the theoretical result that nitrogen-split interstitials are the dominant defects in Ga(As,N).¹² We therefore believe that the distinct electron trap Ek1 is associated with a split interstitial defect $(N-N)_{As}$ on an As site. Midgap levels are theoretically predicted for such defects in GaAs.¹³ For the GaN mole fraction of about 0.2%, i.e., for a nitrogen concentration of 5×10^{19} cm⁻³, we find the Ek1 level from curves 8 and 9 in Fig. 1(b) at about $E_C - 0.55$ eV, in accordance with the theoretical results. From the composition range covered by the deep-level spectra 4–9 in Fig. 1, we can estimate that the level Ek1 is fixed to about 0.80 eV above the valence band edge, when the GaN mole fraction is changed. The level remains a deep level also in the alloy.

At biases lower than -5 V, the capacitance of the sample is determined, as usual, by the width of the depletion layer below the MS contact. The electron traps Ek2, Ek3, and Ek4, which are detected in this bias range [see the curves 6–9 in Fig. 1(b)], can be due to defects in the Ga(As,N) layer or in the GaAs region close to the Ga(As,N)-on-GaAs interface. They are likely associated with intrinsic defects created during MBE growth, which is modified by the rf plasma cell. These electron traps are usually not present in GaAs grown under standard MBE conditions [see curves 1 and 10 in Fig. 1(b)].

Deep-level spectra of the aforementioned GaAs/Ga(As,N)/GaAs structure after annealing are displayed in Fig. 4. The concentration of the electron trap Ek1 in Ga(As,N) is dramatically reduced by rapid thermal annealing. The underlying defect is obviously annihilated by reactions between intrinsic defects. Reactions with As vacancies, for example, can lead to a dissociation of the nitrogen-split interstitial defect $(N-N)_{As}$ accompanied by the generation of two substitutional N_{As} sites. Such an increase of the N_{As} density after annealing has actually been observed in Ga(As,N).⁴ The level Ek3 is missing after annealing. The traps Ek2 and Ek4 are detected in different bias regions [see Fig. 4(b)], i.e., they occur in Ga(As,N) and GaAs, respectively. Because Ek4 is similar to the well-known EL2 level in GaAs,¹⁰ it is suggested that Ek2 is due to the same antisite defect on Ga site in Ga(As,N) as the EL2 level in GaAs. The antisite defect in Ga(As,N) has been also identified by optically detected magnetic resonance.¹⁴

In conclusion, electron traps have been examined in strained Ga(As,N) with 3% GaN mole fraction. We find in as-grown samples a giant concentration of an electron trap at

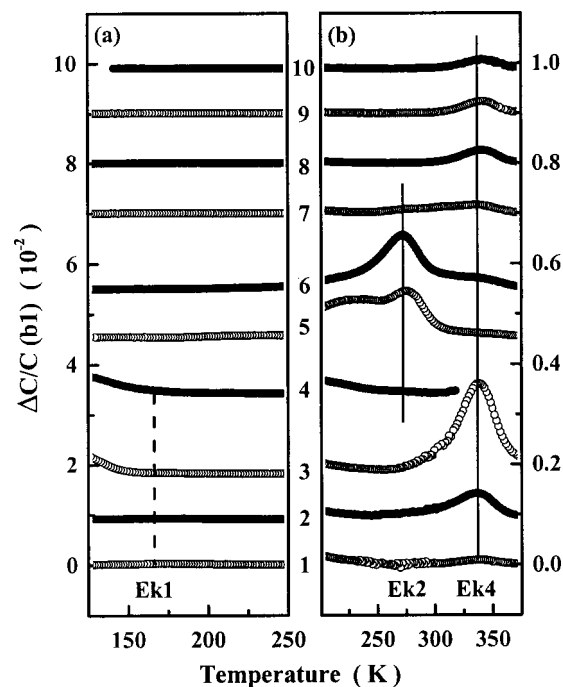


FIG. 4. Deep-level spectra for the same n -type heterostructure as in Fig. 1, but after postgrowth annealing. Measuring conditions for the spectra 1–10 are identical to those in Fig. 1. Note the same scales as in Fig. 1.

$E_C - 0.25$ eV, which is probably connected with a nitrogen-split interstitial defect on an As site. The concentration of this distinct trap can be strongly reduced by annealing. Since the capture cross section of this level is about 10^{-17} cm², it can not be the recombination center, which causes the degradation of the luminescent properties of Ga(As,N) at larger GaN mole fractions.

The authors would like to thank H. T. Grahn for helpful comments and a careful reading of the manuscript. They are grateful for the technical assistance of H. Kostial and E. Wiebicke.

¹M. Weyers, M. Sato, and H. Ando, Jpn. J. Appl. Phys., Part 2 **31**, L853 (1992).

²P. Krispin, S. G. Spruytte, J. S. Harris, and K. H. Ploog, J. Appl. Phys. **90**, 2405 (2001).

³P. Krispin, S. G. Spruytte, J. S. Harris, and K. H. Ploog, J. Appl. Phys. **88**, 4153 (2000).

⁴S. Francoeur, G. Sivaraman, Y. Qiu, S. Nikishin, and H. Temkin, Appl. Phys. Lett. **72**, 1857 (1998).

⁵E. V. K. Rao, A. Ougazzaden, Y. Le Bellego, and M. Juhel, Appl. Phys. Lett. **72**, 1409 (1998).

⁶A. Moto, S. Tanaka, N. Ikoma, T. Tanabe, S. Takagishi, M. Takahashi, and T. Katsuyama, Jpn. J. Appl. Phys., Part 1 **38**, 1015 (1999).

⁷S. G. Spruytte, C. W. Coldren, A. F. Marshall, M. C. Larson, and J. S. Harris, Mater. Res. Soc. Symp. Proc. **595**, W8.4.1 (2000).

⁸P. Krispin, S. G. Spruytte, J. S. Harris, and K. H. Ploog, J. Appl. Phys. **89**, 6294 (2001).

⁹S. Weiss and R. Kassing, Solid-State Electron. **31**, 1733 (1988).

¹⁰D. Pons, Appl. Phys. Lett. **37**, 413 (1980).

¹¹S. G. Spruytte, C. W. Coldren, J. S. Harris, W. Wampler, P. Krispin, K. Ploog, and M. C. Larson, J. Appl. Phys. **89**, 4401 (2001).

¹²S. B. Zhang and S. H. Wei, Phys. Rev. Lett. **86**, 1789 (2001).

¹³J. E. Lowther, S. K. Estreicher, and H. Temkin, Appl. Phys. Lett. **79**, 200 (2001).

¹⁴N. Q. Thinh, I. A. Buyanova, P. N. Hai, W. M. Chen, H. P. Xin, and C. W. Tu, Phys. Rev. B **63**, 033203 (2001).